

Electronic Supplementary Information for

Dependence of Crystal Size on the Catalytic Performance of a Porous Coordination Polymer

Tomokazu Kiyonaga,^a Masakazu Higuchi,^{a,b} Takashi Kajiwara,^a Yohei Takashima,^a
Jingui Duan,^a Kazuro Nagashima^c and Susumu Kitagawa^{*ad}

^a Institute for Integrated Cell-Material Sciences (iCeMS), Kyoto University, Yoshida Ushinomiya-cho, Sakyo-ku, Kyoto 606-8501, Japan.

^b Japan Science and Technology Agency, PRESTO, 4-1-8 Honcho, Kawaguchi, Saitama 332-0012, Japan.

^c Shoei Chemical Inc., 5 Azawakasa, Fujikicho, Tosu, Saga 841-0048, Japan.

^d Department of Synthetic Chemistry and Biological Chemistry, Graduate School of Engineering, Kyoto University, Kyoto-daigaku Katsura, Nishikyo-ku, Kyoto 615-8510, Japan.

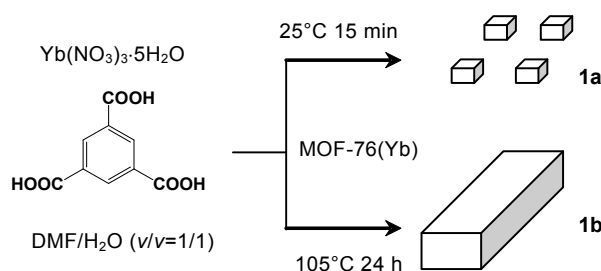
kitagawa@icems.kyoto-u.ac.jp

Experimental Section

General Remarks. Morphological features were examined by scanning electron microscope (JSM-5600, JEOL). X-ray powder diffraction (XRPD) data were collected on a Bruker AXS D8 DISCOVER with GADDS. Data were collected over the 2θ range from 4.00° to 40.20° in 0.02° steps via 600 sec scans, with Cu $K\alpha$ radiation ($\lambda = 1.54184 \text{ \AA}$). Thermogravimetric analyses (TGA) were performed on a RIGAKU Thermo plus EVO II TG8120, using a heating rate of 5 K min^{-1} under an N_2 atmosphere. Gas sorption isotherm measurements were performed with a BEL Japan BELSORP-max. IR spectra were recorded on a Thermo Fisher Scientific Nicolet 6700 spectrometer.

Materials. All reagents and solvents used for the synthesis of PCPs are commercially available and were used as received without further purification.

Synthesis of $\text{MOF-76(Yb)} \cdot (\text{H}_2\text{O}) \cdot (\text{DMF})_{1.1}$.



Scheme 1. Synthesis of **1a** and **1b**.

The nanosized $\text{MOF-76(Yb)} \cdot (\text{H}_2\text{O}) \cdot (\text{DMF})_{1.1}$ (denoted as **1a** \supset solv) was successfully synthesized as follows: A mixture of $\text{Yb}(\text{NO}_3)_3 \cdot 5\text{H}_2\text{O}$ (0.625 mmol) and sodium formate (0.625 mmol) were dissolved in DMF (5 mL) and H_2O (5 mL). The 1,3,5-benzenetricarboxylate (H_3BTC , 0.625 mmol) in DMF (5 mL) and H_2O (5 mL) was added to the ytterbium solution, and the mixture was stirred at room temperature for 15 min. The conventionally synthesized $\text{MOF-76(Yb)} \cdot (\text{H}_2\text{O}) \cdot (\text{DMF})_{1.1}$ (denoted as **1b** \supset solv) was synthesized by solvothermal synthesis.^{S1} A mixture of $\text{Yb}(\text{NO}_3)_3 \cdot 5\text{H}_2\text{O}$ (0.625 mmol) and H_3BTC (0.625 mmol) were dissolved in DMF (5 mL) and H_2O (5 mL), and the sealed reaction mixture was then placed in the oven and heated to 105°C for 24 h. These resulting **1a** and **1b** were recovered from the milky suspension by centrifugation, washed with DMF several times, and dried using a vacuum pump.

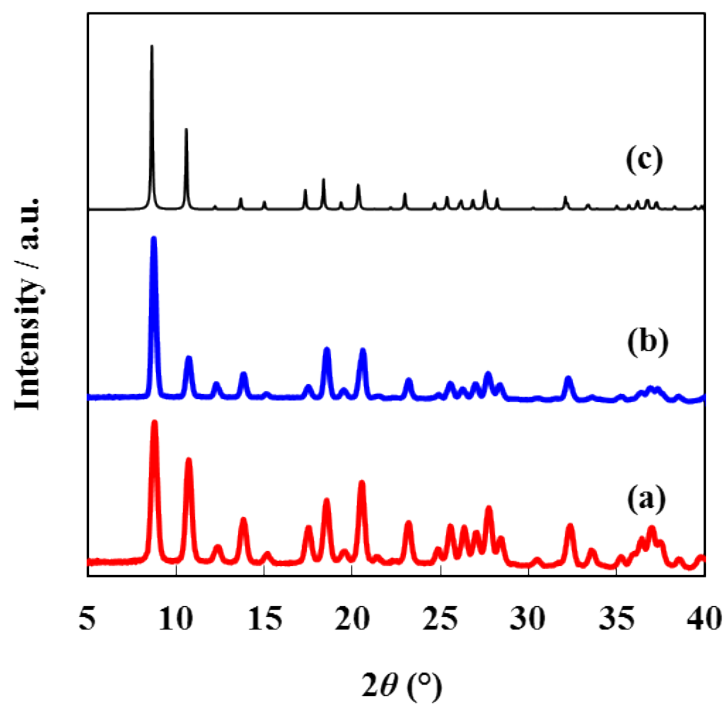


Fig. S1 The XRPD patterns of MOF-76(Yb): (a) **1a**; (b) **1b**; (c) simulated MOF-76(Yb).

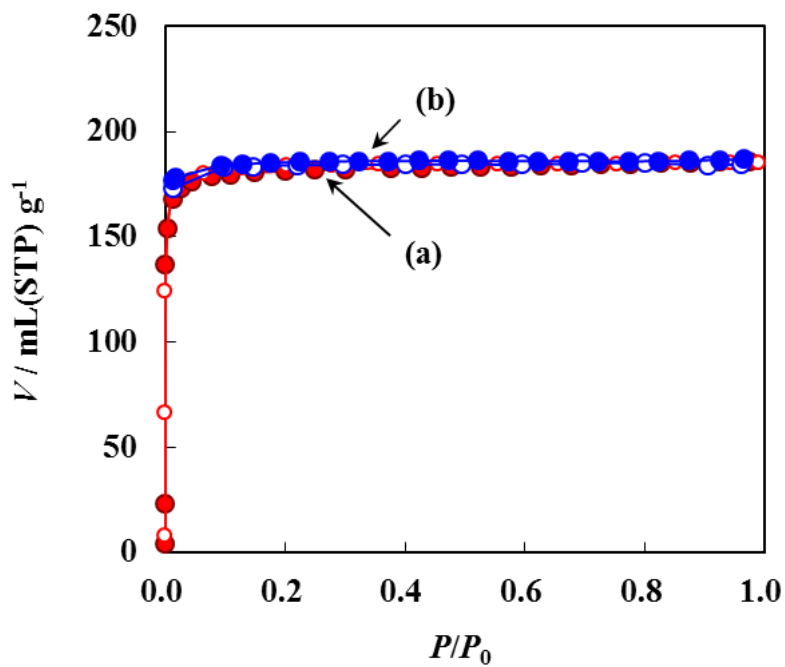


Fig. S2 N₂ sorption isotherms of (a) **1a** and (b) **1b** at -196°C: ●, adsorption; ○, desorption.

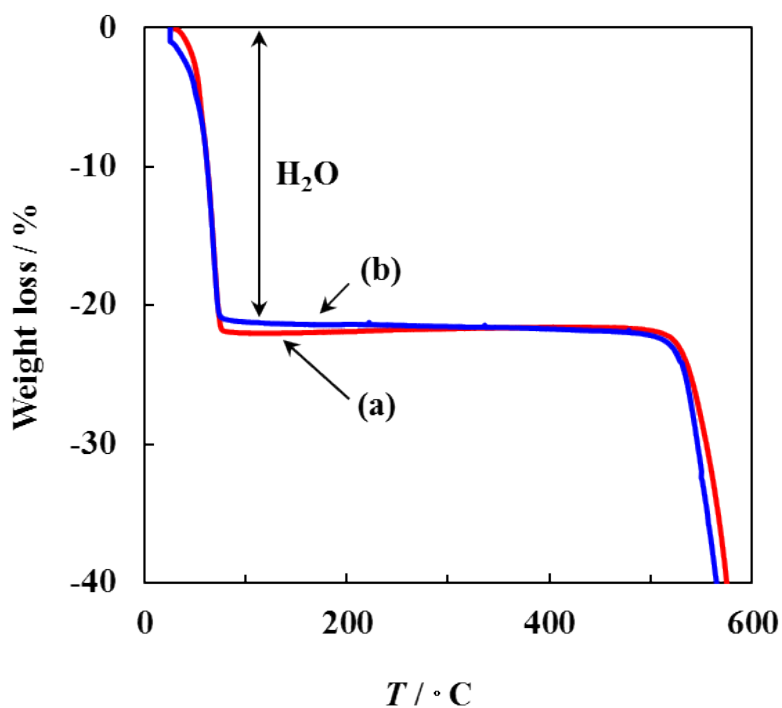


Fig. S3 TGA profiles of (a) **1a** and (b) **1b**.

Discussion on the IR Spectra. As seen in Fig. S4, the carbonyl stretching vibration peak (without shoulder) was observed in the acetone-adsorbed PCPs. This phenomenon indicates that there is one kind of acetone molecules interacting with acidic sites. This is in agreement with the type of acidic site in MOF-76. The influence of lanthanide ion species in MOF-76 was also evaluated. The PCP/MOFs showed the same low-frequency shift, indicating an identical degree of acidity (Fig. S5).

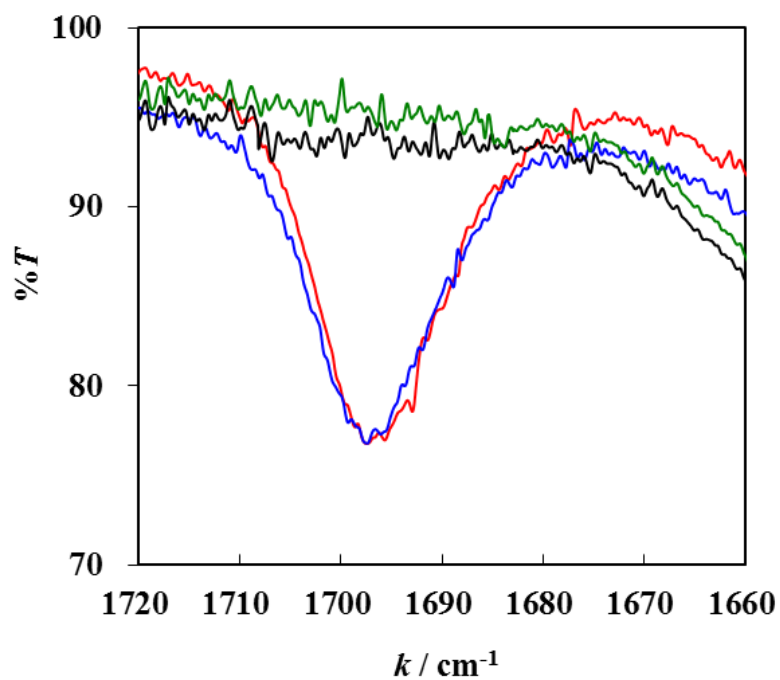


Fig. S4 IR spectra of activated and acetone-adsorbed PCPs: (black) **1a**; (green) **1b**; (red) acetone-adsorbed **1a**; (blue) acetone-adsorbed **1b**.

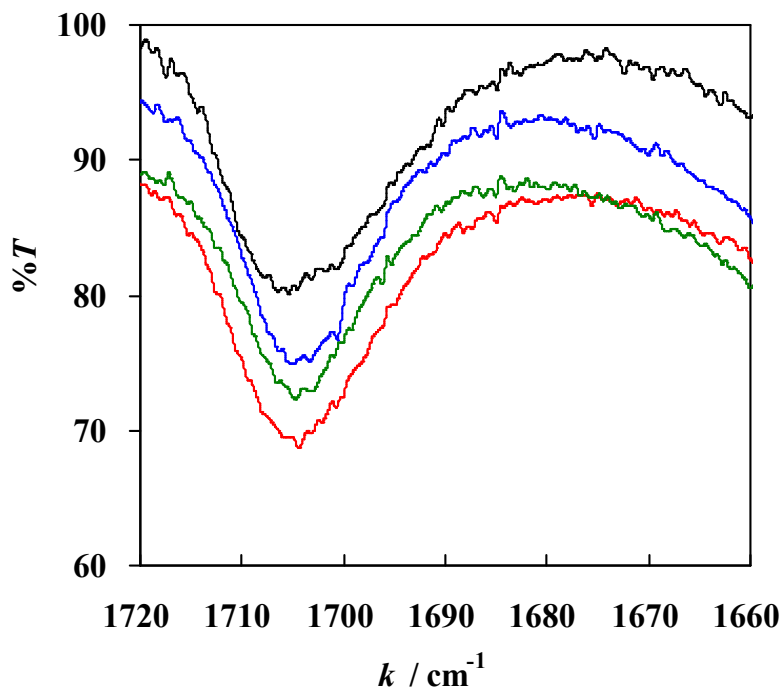


Fig. S5 IR spectra of acetone-adsorbed MOF-76: (black) MOF-76(Tb); (blue) MOF-76(Dy); (green) MOF-76(Er); (Red) MOF-76(Yb).

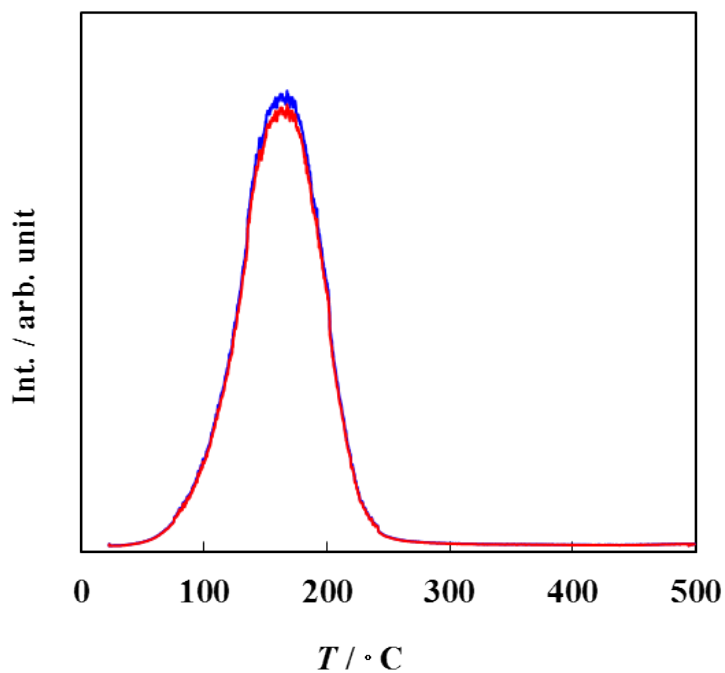


Fig. S6 NH₃-TPD profiles of **1a** (red) and **1b** (blue). The TPD data were collected using a heating rate of 5 K min⁻¹ under He (30 mL min⁻¹) with Q-mass ($m/z = 16$) as a detector.

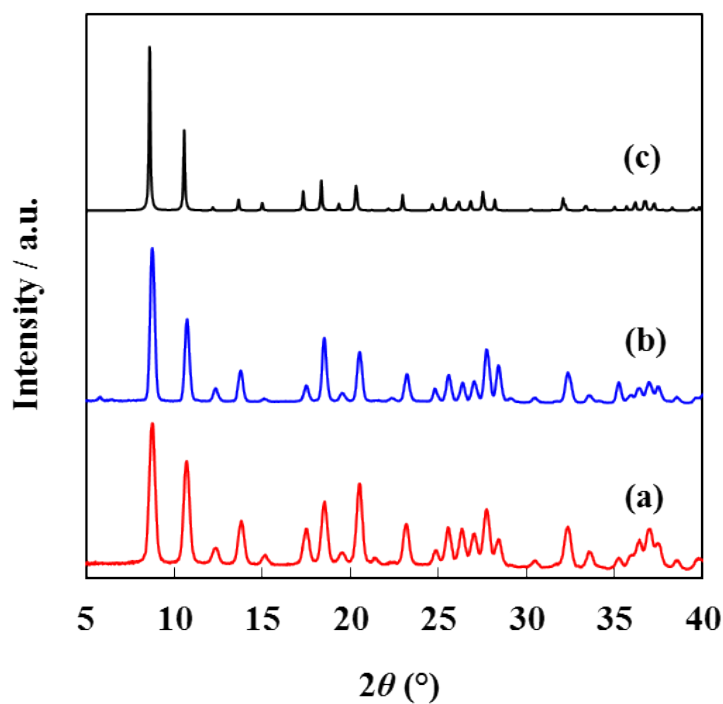


Fig. S7 The XRPD patterns of **1b**: (a) before measurement of NH₃-TPD; (b) after measurement of NH₃-TPD; (c) simulated MOF-76(Yb).

Esterification reaction of acetic acid with methanol. The vessel was charged with activated catalyst (0.22 mmol), acetic acid (1.3 mmol), and methanol (45 mmol) (substrate:catalyst=6:1). The reaction mixture was heated at 100°C by microwave irradiation (microwave synthesizer, Biotage). The product was analyzed by the gas chromatograph (GC-2014, Shimadzu) using capillary column with flame ionization detector. The results are summarized in Fig. 2.

Esterification reaction of a benzoic acid with methanol. The vessel was charged with activated catalyst (0.22 mmol), benzoic acid (1.3 mmol), and methanol (45 mmol) (substrate:catalyst=6:1). The reaction mixture was heated for 1h at 100°C by microwave irradiation (microwave synthesizer, Biotage). The product was analyzed by the gas chromatograph (GC-2014, Shimadzu) using capillary column with flame ionization detector. The results are summarized in Table S1.

Confirmation of the encapsulation of the substrates (acetic acid and benzoic acid). The vessel was charged with activated catalyst (0.22 mmol), carboxylic acids (0 - 7.8 mmol), and methanol (45 mmol) (substrate:catalyst=6:1). The mixture was stirred at room temperature for 12 h. The absorbed amount of carboxylic acids was analyzed by the gas chromatograph (GC-2014, Shimadzu) using capillary column with flame ionization detector. The results are summarized in Fig. S8.

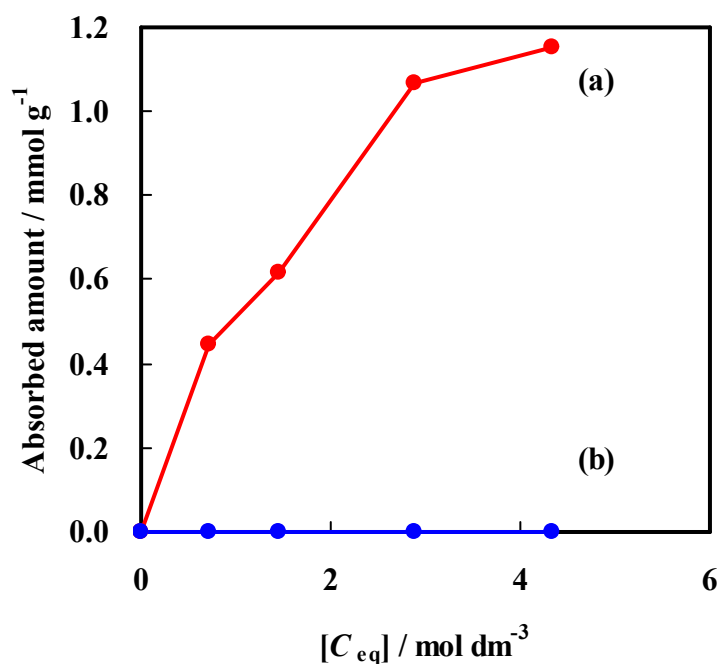


Fig. S8 Sorption isotherms of (a) acetic acid and (b) benzoic acid on **1a**.

Table S1 Microwave assisted esterification reaction of benzoic acid with methanol.

Catalyst	Crystal size / μm	Yield (%)
1a	0.8	0.3
1b	50	0.3
without catalyst	—	0.3

Comparison of the catalytic activity. To compare the catalytic activity of **1a** and **1b** with those of known PCPs, the reported results are summarized in Table S2. Because the reaction conditions are different in each literature, the comparison of the yields is not appropriate. Therefore, we have calculated the TOF values for the comparison. TOF was standardized by total amount of acid. When the catalytic active site is not perfectly performed, the calculated TOF is underestimated.

Table S2 Comparison of the catalytic activity of PCPs in various reactions.

Catalyst	Dimension	Reaction	Acid amount /mmol g ⁻¹	Crystal size / μm	Yield (%)	TOF ^a / h ⁻¹	Ref
1a	1D	Esterification reaction ^b	2.63 ^f	0.8	47	2.6	This work
1b	50			15	0.8		
MOF-74(Co)	1D	Cycloaddition of CO ₂ to styrene oxide ^c	6.39 ^g	50	54	21	S6
				300	51	20	
UiO-66	3D	Cyclization of (+)-citronellal ^d	2.40 ^h	0.050	78	0.20	S7
				0.300	82	0.21	
MIL-101(Cr)	3D	Oxidation of diphenyl methane ^e	4.40 ⁱ	0.060	10	0.54	S8
				0.400	12	0.65	

^a TOF = (yield)/(total amount of acid)/(t). ^b AcOH:MeOH= 1:35, 5.32 w% cat., 100°C 1h, $P=0.1$ MPa). ^c styrene oxide: chlorobenzene=1:59, 0.06 w% cat., 100°C, 2h, $P_{\text{CO}_2}=2.0$ MPa. ^d citronellar : toluene = 1:104, 1.7 w% cat., 100°C, 1h, $P=0.1$ MPa. ^e DPM: *t*-butyl-hydro- peroxide (TBHP) : acetonitrile=1:1.75: 129, 0.74 w% cat., 150°C, 7 min, $P=0.1$ MPa. ^f ref. S1. ^g ref. S3. ^h ref. S4. ⁱ ref. S5.

Isomerization reaction of 1-Hexene. The isomerization reaction of 1-hexene was conducted by utilizing the apparatus shown in Fig. S8.^{S9} The sample (0.13 mmol) was loaded in a glass insert [b] and activated at 400 °C for 5 min under a flow of He. After the pretreatment, the stop valves [e] were closed and 1-hexene (0.80 mmol) was added via INJ-1 (substrate:catalyst=6:1). 1-Hexene was allowed to react in the closed reaction system at 400°C. Then the six port valve [a] was switched to the dashed lines. The reaction mixture was analyzed by the GC using capillary [c] and packed columns [d] with FID as a detector. The product distribution is summarized in Table S3.

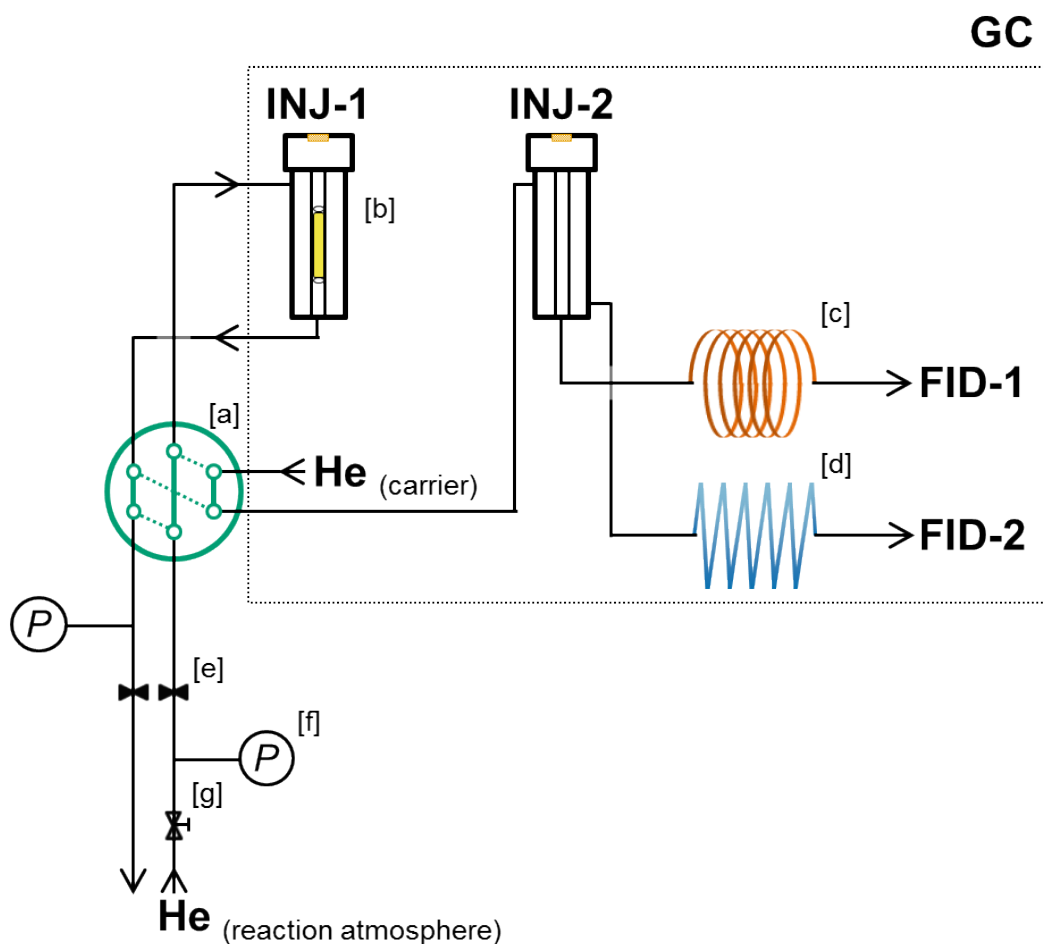


Fig. S9 Schematic representation of the apparatus for the reaction of 1-hexene: [a] six port valve; [b] catalyst loaded inside a glass insert; [c] capillary column; [d] packed column; [e] stop valve; [f] pressure gauge; [g] pressure control valve.

Table S3 Distribution of the reaction mixture of 1-hexene under different heating times.

Product	30 s			60 s			120 s		
	none	1a	1b	none	1a	1b	none	1a	1b
cracking products (C ₁₋₅ hydrocarbon)	0.13	0.28	0.32	0.13	0.35	0.41	0.18	0.39	0.39
isomerization products (C ₆ hydrocarbon)	1.15	3.40	3.18	1.40	4.09	4.07	1.77	5.35	5.35
unreacted substrate (1-hexene)	98.7	96.3	96.5	98.4	95.5	95.5	98.0	94.2	94.2
other products (C ₇₊ and aromatics)	0.04	0.06	0.03	0.04	0.05	0.04	0.08	0.09	0.09

Preparation of MOF-76(Yb)/ γ -Al₂O₃. The composite of PCP and other materials provide the a variety of possibility.^{S10} Hence, we challenged the preparation of the composite of MOF-76(Yb) and the catalyst support (γ -Al₂O₃). The MOF-76(Yb)/ γ -Al₂O₃ were prepared by the solvothermal synthesis. A mixture of Yb(NO₃)₃ · 5H₂O (0.625 mmol) and H₃BTC (0.625 mmol) were dissolved in DMF (5 mL) and H₂O (5 mL), and then γ -Al₂O₃ (10.0 g) was added to the reaction mixture. The sealed reaction mixture was then heated in the oven (105°C, 24 h). This resulting sample was recovered by filtration, washed with DMF several times, and dried using a vacuum pump. The X-ray diffraction (XRD) data were collected on Shimadzu XRD-7000 using Polycapillary Parallel Beam Optics. Data were collected over the 2 θ range from 5.00° to 40.00° in 0.02° steps via 1050 sec scans, with Cu K α radiation ($\lambda = 1.54060$ Å). As shown in Fig. S10, the polycapillary XRD pattern of the sample was very close to each other and were in good agreement with the pattern of MOF-76(Yb).^{S1} The layer thickness of MOF-76(Yb) shell was 3 μ m, the rod-shaped particle was agglomerated on the surface of γ -Al₂O₃ (Fig. S11). Thus, MOF-76(Yb) could be successfully deposited on γ -Al₂O₃.

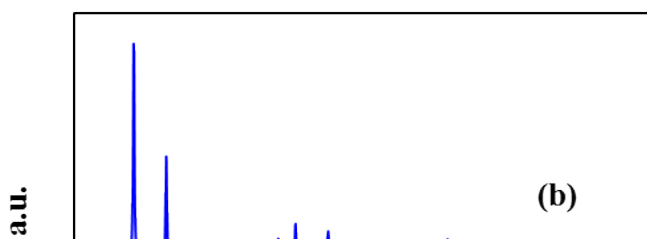


Fig. S10 The polycapillary XRD patterns of (a) MOF-76(Yb)/ γ -Al₂O₃ and (b) simulated MOF-76(Yb).

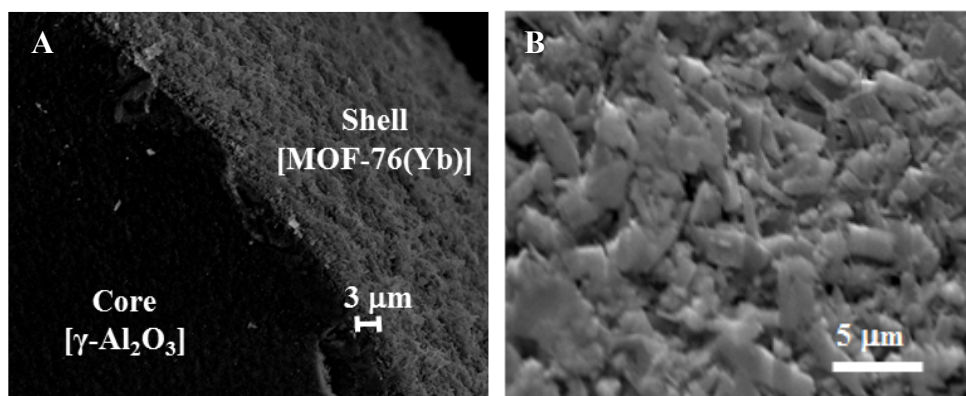


Fig. S11 The cross-sectional SEM images (A) and the surface SEM image (B) of MOF-76(Yb)/ γ -Al₂O₃.

References

- S1 H. L. Jiang, N. Tsumori, and Q. Xu, *Inorg. Chem.*, 2010, **49**, 10001.
- S2 X. Guo, G. Zhu, Z. Li, F. Sun, Z. Yang and S. Qiu, *Chem. Commun.*, 2006, 3172.
- S3 P. D. C. Dietzel, Y. Morita, R. Blom, and H. Fjellvag, *Angew. Chem. Int. Ed.*, 2005, **44**, 6354.
- S4 J. H. Cavka, S. Jakobsen, U. Olsbye, N. Guillou, C. Lamberti, S. Bordiga, and K. P. Lillerud, *J. Am. Chem. Soc.*, 2008, **130**, 13850.
- S5 N. A. Khan, In J. Kang, H. Y. Seok, S. H. Jung, *Chem. Eng. J.*, 2011, **166**, 1152.
- S6 H. Y. Cho, D. A. Yang, J. Kim, S. Y. Jeong and W. S. Ahn, *Catal. Today*, 2012, **185**, 35.
- S7 F. Vermoortele, M. Vandichel, B. V. Voorde, R. Ameloot, M. Waroquier, V. V. Speybroeck and D. E. Vos, *Angew. Chem. Int. Ed.*, 2012, **51**, 4887.
- S8 A. Dhakshinamoorthy, M. Alvaro, Y. K. Hwang, Y. K. Seo, A. Corma and H. Garcia, *Dalton Trans.*, 2011, **40**, 10719.
- S9 T. Kajiwara, M. Higuchi, A. Yuasa, H. Higashimura and S. Kitagawa, *Chem. Commun.*, 2013, DOI:10.1039/C3CC43384F.
- S10 S. Aguado, J. Canivet, Y. Schuurman and D. Farrusseng, *J. Catal.*, 2011, **284**, 207.